# Investigation of Electrical Stimulus on Chitosan Film Based DDS

Md Nazmus Sahadat[1], *Student Member, IEEE, EMBS,* Alex P. Hoban[2], Bashir I. Morshed[1], *Member, IEEE, EMBS* and Warren O. Haggard[2]

***Abstract*— Controlled drug release is crucial for targeted implant smart drug delivery system (DDS). In this work a chitosan film loaded with green food coloring is fabricated to demonstrate the concepts of drug release using electrical stimulus. A simulation model is also developed to explain the physical phenomena of this drug release using finite element method (FEM). It is found that drug delivery is increased with applied electric field to the electrodes on chitosan film. The AC electrokinetic force generated from electrical excitation is a factor influencing this phenomenon. Several controlled and stimuli experiments are conducted with different electric fields and frequencies. The spectral absorbance of treated solution after the experiment is measured using a spectrophotometer to quantify the dye release. It is verified statistically with 99% level of significance that the amount of dye release has increased with applied electric field. Thus this work has shown that application of electric field can be a potential candidate for controlled DDS using chitosan film.**

## I. INTRODUCTION

Over many years research effort has been directed towards safe and efficient targeted controlled drug delivery system (DDS). The application of chitosan for this kind of drug delivery has been increasingly investigated over past decade. Many researchers are focusing particularly on chitosan based biomaterial delivery because of it's unique material property. Chitosan is compatible with many therapeutic agents and degradable. It breaks down slowly to harmless by-products(amino sugars) which are completely absorbed by the human body [1]. Chitosan degrades under the action of liposome, nontoxic and easily removable from the organism without causing concurrent side reactions. It possesses antimicrobial property and absorbs toxic metals like mercury, cadmium, lead, etc. In addition, it has good adhesion, coagulation ability, and immunostimulating activities [2].

Chitosan also has multiple applications in drug delivery system (DDS). In 2004, Agnihotri *et al.* has mentioned about different techniques of preparing chitosan, loading drug and controlled release. This type of DDS has application in colon, cancer therapy, gene delivery, multiple topical and ocular delivery systems [2]. *Vivek et al.* has shown chitosan based DDS for breast cancer therapy application [3]. In 2001, Illum *et al.* has discussed about different chitosan based influenza, pertussis, diptheria vaccines applications [4]. Kang *et al.* has mentioned about chitosan microspheres for nasal delivery [5]. In 2003, Illum *et al.* has given an idea to deliver chitosan based drug to brain tissue through olfactory using nasal path [6]. Ribeiro *et al.* created a pectin coated chitosan beads for colon targeted drug delivery that can release drug based upon pH change [7]. In 2014, Zhang *et al.* has created a Cytocompatible injectable pH and temperature controlled DDS [8]. Luo *et al.* has discussed about Nano/micro particle, hydrogel beads, layer by layer film based chitosan DDS system [9]. Kusrini *et al.* has modified chitosan using samarium to improve drug release [10]. Bernkop-Schnrch *et al.* has discussed about the cationic nature of chitosan for controlled drug delivery applications. They have also mentioned different chitosan based DDS over the past 20 years [11].

All these delivery system mentioned above are based upon pH or temperature controlled by the inner environment of human body. In this work, we have demonstrated electrical stimulation based drug release which can be controlled outside from the body. The main contribution of this work is the amount of drug like agent release demonstration with respect to time and controllability by changing electric field using chitosan film.

## II. THEORY

AC electrokinetic forces can generate swirling patterns in the fluid and thereby enhance the transport of the analyte to the reaction surface [12]. The AC electrokinetic forces arise when the fluid absorbs energy from an applied nonuniform AC electric field by means of Joule heating. The temperature increase changes the fluid's conductivity and permittivity. Consequently the fluid experiences an effective or time-averaged volume force, which depends on the conductivity and permittivity gradients and on the field intensity. By changing the shape of the electric field it is possible to alter this force which will cause the velocity change to the fluid. This velocity change will increase the diffusion of drug from chitosan film. It can also create breakage on the film to release drug [13].

Three different physics are used to explain this phenomena. Fluid flow in the channel follows the Navier-Stokes theorem:

$$\rho \frac{\partial \mathbf{u}}{\partial t} - \eta \nabla^2 \mathbf{u} + \rho \mathbf{u} \cdot \nabla \mathbf{u} + \nabla p = \mathbf{F} \tag{1}$$

$$\nabla \cdot \mathbf{u} = 0 \tag{2}$$

where $\mathbf{u}$ denotes the velocity, $\rho$ is the density, $\eta$ is the dynamic viscosity, and $p$ refers to the pressure.

*This work is supported by FedEX Innovation Grant(2012-537865).

[1]Md Nazmus Sahadat and Bashir I. Morshed are with Department of Electrical and Computer Engineering.

[2]Alex Prentice Hoban and Warren O Haggard are with the Department of Biomedical Engineering, University of Memphis, Memphis, TN 38152, USA.

978-1-4244-7929-0/14/$26.00 ©2014 IEEE

The volume force **F** appearing in the equation is the AC electrokinetic force:

$$\mathbf{f}_E = -0.5[(\frac{\nabla\sigma}{\sigma} + \frac{\nabla\varepsilon}{\varepsilon})\cdot\mathbf{E}\frac{\varepsilon\mathbf{E}}{1+(\omega\tau)^2} + 0.5|\mathbf{E}|^2\nabla\varepsilon \quad (3)$$

where $\sigma$ is the conductivity, $\varepsilon = \varepsilon_r\varepsilon_0$ equals the fluid permittivity, $\omega$ represents the electric field's angular frequency, and $\tau = \varepsilon/\sigma$ gives the fluid charge-relaxation time. The field vector **E** contains the amplitude and orientation of the AC electric field but not its instantaneous value. Volume force contains two different forces. The first part of (3) is coulomb's force and the second part due to dielectric force. This force can be controlled by changing both electric field and frequency of the applied stimuli.

$\varepsilon$ and $\sigma$ will change because of the temperature rise resulted from Joule heating. So We can rewrite the gradients of these parameters using partial differentiation, which yields (4) and (5)

$$\nabla\varepsilon = (\frac{\partial\varepsilon}{\partial T})\nabla T \quad (4)$$

$$\nabla\sigma = (\frac{\partial\sigma}{\partial T})\nabla T \quad (5)$$

where $T$ is the fluid temperature. For water (4) and (5) become (6) and (7).

$$(\frac{\partial\varepsilon}{\partial T})\nabla T = -0.004K^{-1} \quad (6)$$

$$(\frac{\partial\sigma}{\partial T})\nabla T = -0.02K^{-1} \quad (7)$$

Thus the electrothermal force (3) can be rewritten as (8).

$$\mathbf{f}_E = -0.5\varepsilon((0.016K^{-1})\nabla T\cdot\mathbf{E}\frac{\mathbf{E}}{1+(\omega\tau)^2} + 0.5|E|^2(-0.004K^{-1}\nabla T)) \quad (8)$$

Electrothermal force is a time-averaged entity. So we can solve the static electric field that corresponds to the root mean square (rms) value of the AC field. To solve the electric current problem, turn to following equations (9-11).

$$-\nabla\cdot\mathbf{J} = Q_j \quad (9)$$

$$\mathbf{J} = -\sigma\mathbf{E} + \mathbf{J_e} \quad (10)$$

$$\mathbf{E} = -\nabla V \quad (11)$$

where **E**, **J** and **V** are electric field, current density and electric potential.

## III. Modeling

The whole system is modeled considering one pair of electrodes ($1016\mu m \times 2\mu m$) with chitosan film ($0.6096mm \times 0.5mm$) at the bottom and a cavity($0.6096mm \times 0.5mm$) with water as fluid. A cross section of the whole system is considered for the simplicity of modeling. Periodic condition on both sides of the electrodes are assumed to include the effect of other electrodes of the interdigited configuration. Electric current, laminar flow and heat transfer physical laws are included to solve this system using COMSOL multiphysics (COMSOL, Inc, Palo Alto, CA, USA). Extra fine physics controlled meshes are generated to obtain the results in two steps. First electric current is solved in stationary domain. Then heat transfer and laminar flow problems are solved in time domain by using the solution from first step. Finally Electric field, potential, velocity, pressure, volume force and temperature rise results are found using finite element method by combining those two stationary and time domain solutions. The boundary conditions of the above mentioned physics are given in tables I to III.

TABLE I: Boundary conditions for electric current problem

| BOUNDARY | CONDITION |
|---|---|
| Left Electrode | Electric potential $V = V_{rms}$ |
| Right Electrode | Electric potential $V = -V_{rms}$ |
| Left, Right Cavity | Periodic condition |
| Top, Bottom | Electric insulation |

TABLE II: Boundary conditions for heat transfer

| BOUNDARY | CONDITION |
|---|---|
| Left, Right Electrodes | Heat Sources |
| Left, Right Cavity | Periodic heat condition |
| Top | Ambient temperature |
| Bottom | Heat insulation |

## IV. Chitosan Film Preparation

A chitosan solution, 1% v/v Lactic Acid, 1% w/v chitosan (Chitopharm S), approximately 13 drops per liter green food coloring, was added (100ml) to a 9 cm diameter glass petri dish. This chitosan solution in the petri dish was allowed to dry non covered in normal laboratory conditions for 3-5 days depositing a chitosan film contain green food coloring on the inside and bottom of the petri dish. Approximately 100ml of a neutralizing solution, 80% v/v ethanol and 2% w/v sodium hydroxide, was added to the petri dish containing the chitosan film to neutralize the film. The film was left to neutralize in the neutralizing solution for 30 minutes. Then, the neutralizing solution was removed and the wet, neutralized chitosan film in the petri dish was left to dry uncovered in normal laboratory conditions for 2-3 hours.

## V. Experiments

This neutralized loaded dye chitosan film is used as a model to observe the drug release phenomena in vitro. Two different types of experiments were done. One of them was controlled, without using any electrical excitation and another was with electrical excitation. Both the controlled and electrical excitation were applied for 15 minutes. $500\mu L$ deionized water was used to do the experiments. Different voltages and frequency electrical pulses were tried to observe dye release. Samples were collected after each experiment. The setup of the experiment is shown Fig. 1

## VI. Results

### A. Simulation Results

Electric field, velocity of the fluid and temperature profile are obtained from finite element method (FEM). Electric field

TABLE III: Boundary conditions for laminar flow

| BOUNDARY | CONDITION |
|---|---|
| Left Cavity | Normal inflow velocity |
| Right Cavity | Normal outflow velocity |
| Top, Bottom Cavity | Wall (No slip) |

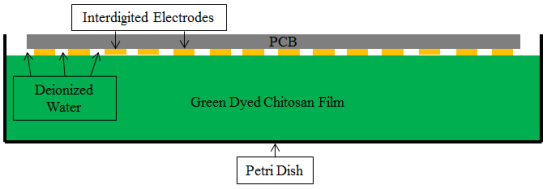


Fig. 1: Experimental setup for electrical stimuli

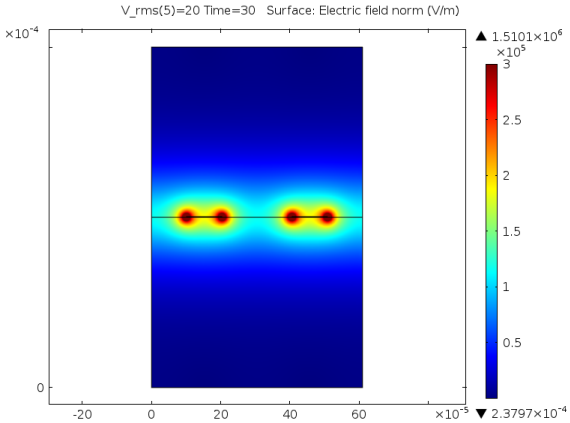


Fig. 2: Electric field distribution inside of the model

at the corner of the electrodes are high. This is shown in Fig. 2. Maximum volume force is produced at two corners of the electrodes. But at the middle of the electrode, force is lower. Volume force difference creates a pressure gradient which causes a swirling pattern fluid flow inside of the cavity. Fig. 3 shows the swirling fluid velocity pattern. Here surface plot shows the amplitude of the velocity and velocity field is shown by arrow surface. A swirling pattern can be observed from the direction of arrow surface. Temperature rise inside of the chamber is shown in Fig. 4. Although temperature is maximum at the electrodes but the amount of rise is very less ($8.9 \times 10^{-9} K$). It also gradually decreases towards the ambient which is important for implanted device.

The effect of voltage on volume force is presented in Fig. 5. It can be observed that volume force increases with electric potential at two corner points (6,7) of the electrode. But force has a little effect with the change of excitation frequency which is shown in Fig. 6.

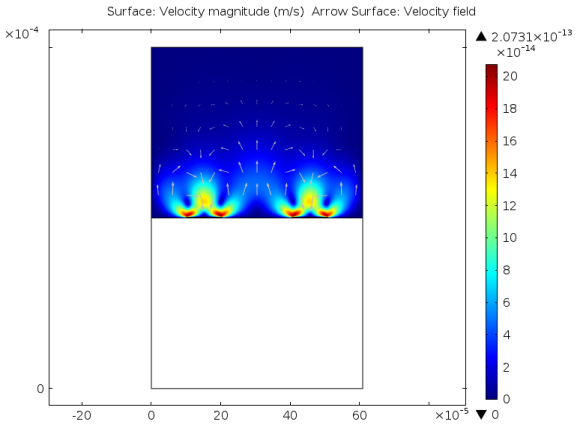


Fig. 3: Fluid velocity inside of the model

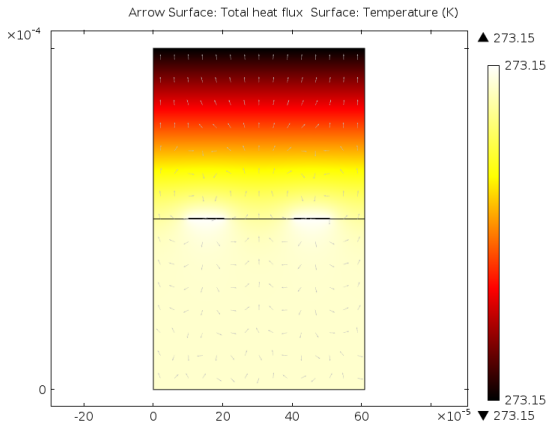


Fig. 4: Temperature and heat flux inside of the model

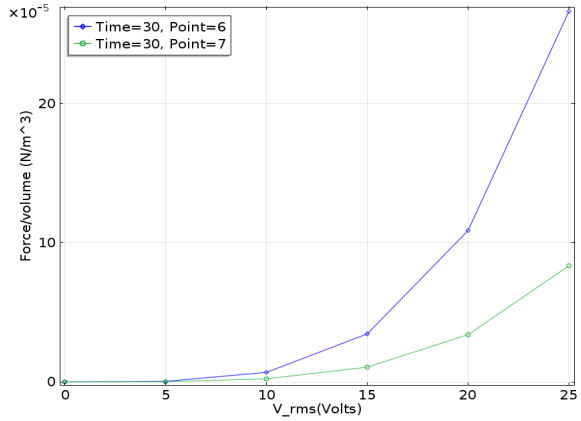


Fig. 5: AC electrokinetic force for different electric potential

### B. Experimental Results

For experiments, different amplitude and frequency bipolar pulses were applied using a signal generator (DG4062, RIGOL, Ohio, USA) to release and quantify dye in terms of absorbance after excitation. This result is compared with the controlled experiment for each set. For different amplitude and frequency the amount of dye release was different. This result is reflected on the absorbance data from the spectrophotometer (Synergy H1 microplate reader, BioTek instruments,Vermont, USA). The sample is scanned over a band of wavelength 330$nm$ to 700$nm$ with an increment of

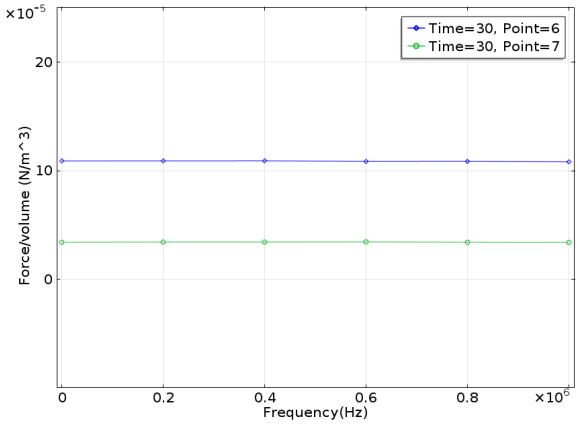


Fig. 6: AC electrokinetic force for different frequency excitation at $V_{rms} = 20V$

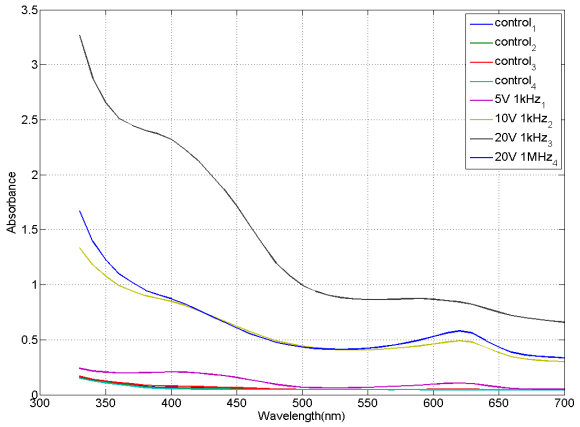


Fig. 7: Mean absorbance for controlled and electrical excitation

TABLE IV: Absorbance for control and excitation experiments

| Exp,Wl(*nm*) | S1 | S2 | S3 | S4 | Mean | STD |
|---|---|---|---|---|---|---|
| C1,400 | 0.068 | 0.072 | 0.067 | 0.054 | 0.065 | 0.008 |
| C1,620 | 0.047 | 0.050 | 0.055 | 0.055 | 0.049 | 0.005 |
| C2,400 | 0.056 | 0.086 | 0.053 | 0.055 | 0.063 | 0.016 |
| C2,620 | 0.045 | 0.050 | 0.043 | 0.044 | 0.046 | 0.003 |
| C3,400 | 0.145 | 0.053 | 0.058 | 0.058 | 0.079 | 0.044 |
| C3,620 | 0.059 | 0.044 | 0.048 | 0.048 | 0.050 | 0.006 |
| C4,400 | 0.048 | 0.057 | 0.057 | 0.056 | 0.055 | 0.004 |
| C4,620 | 0.039 | 0.047 | 0.048 | 0.047 | 0.045 | 0.004 |
| E1,400 | 0.239 | 0.246 | 0.147 | 0.196 | 0.207 | 0.046 |
| E1,620 | 0.113 | 0.117 | 0.081 | 0.113 | 0.106 | 0.017 |
| E2,400 | 1.00 | 0.528 | 1.07 | 0.795 | 0.849 | 0.245 |
| E2,620 | 0.554 | 0.318 | 0.607 | 0.487 | 0.492 | 0.126 |
| E3,400 | 2.25 | 2.22 | 2.28 | 2.53 | 2.32 | 0.141 |
| E3,620 | 0.873 | 0.889 | 0.757 | 0.850 | 0.842 | 0.590 |
| E4,400 | 0.825 | 0.504 | 1.35 | 0.812 | 0.873 | 0.351 |
| E4,620 | 0.562 | 0.361 | 0.851 | 0.548 | 0.581 | 0.202 |

10*nm*. Before the experiment green food color was scanned over that range. Two peaks of absorbance were observed at 400*nm* and 620*nm*. So it is more likely to see absorbance peaks at those wavelengths if there is dye release. Higher absorbance indicates more dye release for that particular excitation. Fig. 7 shows the means absorbance data over a wavelength range 330*nm* to 700*nm*. Here numbers (1 to 4) represent the results from 4 different stimuli. It can be observed that with higher voltage absorbance is more. The absorbance data for 400*nm* and 620*nm* wavelengths (Wl) are summarized in Table IV with mean, standard deviation (STD) for control (C1, C2, C3, C4) and excitation (E1, E2, E3, E4) experiments. The stimuli (E1-E4) used in the experiments are 5V 1kHz, 10V 1kHz, 20V 1kHz and 20V 1MHz. Treated samples (S1, S2, S3, S4) were taken applying same amount of stimuli by repeating each experiment twice for quantification. Sample data did not pass Analysis of variance (ANOVA) test. So two tail Welch's t test is used for 400*nm* and 620*nm* wavelengths to differentiate between control and excitation group [14]. A null hypothesis ($H_0$ : $\mu_0 = \mu_1$) is assumed as: there no effect of excitation on dye release. For 5V 1kHz, 10V 1kHz and 20V 1kHz excitation null hypothesis is rejected with 99% level of significance. 20V 1MHz excitation null hypothesis is also rejected with 95% level of significance. The complete statistical analysis is summarized in Table V with P values.

TABLE V: Statistical analysis results

| Excitation(Wl) | df | $\alpha$ | $t_{crit}$ | $t$ | Decision | P value |
|---|---|---|---|---|---|---|
| 5V1kHz(400*nm*) | 3.18 | 0.01 | 5.84 | 6.12 | Rejected | 0.009 |
| 5V1kHz(620*nm*) | 3.63 | 0.01 | 5.84 | 6.52 | Rejected | 0.007 |
| 10V1kHz(400*nm*) | 3.03 | 0.01 | 5.84 | 6.42 | Rejected | 0.008 |
| 10V1kHz(620*nm*) | 3 | 0.01 | 5.84 | 7.10 | Rejected | 0.006 |
| 20V1kHz(400*nm*) | 3.59 | 0.01 | 5.84 | 30.3 | Rejected | $7.89X10^{-5}$ |
| 20V1kHz(620*nm*) | 3.07 | 0.01 | 5.84 | 26.7 | Rejected | $1.15X10^{-4}$ |
| 20V1MHz(400*nm*) | 3 | 0.05 | 3.18 | 4.67 | Rejected | 0.019 |
| 20V1MHz(620*nm*) | 3 | 0.05 | 3.18 | 5.29 | Rejected | 0.013 |

## VII. CONCLUSIONS

This work shows that the electrical pulses have strong abilities to release drug from chitosan film. Chitosan patch can be used as a carrier for drug delivery inside of human body. This drug release can be controlled by changing the shape of the applied electric field. We have shown the relationship of drug release with pulse amplitude and frequency using simulation and experimental data. Future directions include fabrication of interdigited electrode on the chitosan film and wireless power transfer for controlled drug release in vivo.

## REFERENCES


[1] Nicol, S. *"Life after death for empty shells."* New Scientist 129 (1991): 46-8.

[2] Agnihotri, *et al.,* "Recent advances on chitosan-based micro-and nanoparticles in drug delivery." *Journal of Controlled Release* 100, no. 1 (2004): 5-28.

[3] Vivek, Raju, *et al.,* "Oxaliplatin-Chitosan Nanoparticles Induced Intrinsic Apoptotic Signaling Pathway: A smart Drug Delivery System to Breast Cancer Cell Therapy." *International journal of biological macromolecules* (2014).

[4] Illum, L., *et al.,* "Chitosan as a novel nasal delivery system for vaccines." *Advanced drug delivery reviews* 51, no. 1 (2001): 81-96.

[5] Kang, *et al.,* "Application of chitosan microspheres for nasal delivery of vaccines." *Biotechnology advances* 27, no. 6 (2009): 857-865.

[6] Illum, Lisbeth. "Nasal drug deliverypossibilities, problems and solutions. "*Journal of Controlled Release* 87, no. 1 (2003): 187-198.

[7] Ribeiro, *et al.,* "Pectin-coated chitosanLDH bionanocomposite beads as potential systems for colon-targeted drug delivery." *International journal of pharmaceutics* 463, no. 1 (2014): 1-9.

[8] Zhang, *et al.,* "Cytocompatible injectable carboxymethyl chitosan/isopropylacrylamide hydrogels for localized drug delivery." *Carbohydrate Polymers* 103 (2014): 110-118.

[9] Luo, Yangchao, and Qin Wang. "Recent development of chitosan-based polyelectrolyte complexes with natural polysaccharides for drug delivery." *International journal of biological macromolecules* 64 (2014): 353-367.

[10] Kusrini, *et al.,* "Modification of chitosan by using samarium for potential use in drug delivery system." *Spectrochimica Acta Part A: Molecular and Biomolecular Spectroscopy* 120 (2014): 77-83.

[11] Bernkop-Schnrch, Andreas, and Sarah Dnnhaupt. "Chitosan-based drug delivery systems". *European Journal of Pharmaceutics and Biopharmaceutics* 81, no. 3 (2012): 463-469.

[12] Ramos, A., *et al.,* "Ac electrokinetics: a review of forces in microelectrode structures." *Journal of Physics D: Applied Physics* 31, no. 18 (1998): 2338.

[13] Luo, *et al.,* "Study on the degradation of chitosan by pulsed electric fields treatment." *Innovative food science* & emerging technologies 11.4 (2010): 587-591.

[14] Sawilowsky, Shlomo S, "Fermat, Schubert, Einstein, and Behrens-Fisher: The Probable Difference Between Two Means When $\sigma_1 \neq \sigma_2$". *Journal of Modern Applied Statistical Methods* 1, no.2 (2002): 461472.